Ozone profiles in the high-latitude stratosphere and lower mesosphere measured by the Improved Limb Atmospheric Spectrometer (ILAS)-II: Comparison with other satellite sensors and ozonesondes

T. Sugita,[1] H. Nakajima,[1] T. Yokota,[1] H. Kanzawa,[2] H. Gernandt,[3] A. Herber,[3]
P. von der Gathen,[4] G. König-Langlo,[3] K. Sato,[5] V. Dorokhov,[6] V. A. Yushkov,[6]
Y. Murayama,[7] M. Yamamori,[7] S. Godin-Beekmann,[8] F. Goutail,[9] H. K. Roscoe,[10]
T. Deshler,[11] M. Yela,[12] P. Taalas,[13] E. Kyrö,[14] S. J. Oltmans,[15] B. J. Johnson,[15]
M. Allaart,[16] Z. Litynska,[17] A. Klekociuk,[18] S. B. Andersen,[19] G. O. Braathen,[20]
H. De Backer,[21] C. E. Randall,[22] R. M. Bevilacqua,[23] G. Taha,[24] L. W. Thomason,[25]
H. Irie,[26] M. K. Ejiri,[1,27] N. Saitoh,[28] T. Tanaka,[1] Y. Terao,[29] H. Kobayashi,[30]
and Y. Sasano[1]

[1]   A solar occultation sensor, the Improved Limb Atmospheric Spectrometer (ILAS)-II, measured 5890 vertical profiles of ozone concentrations in the stratosphere and lower mesosphere and of other species from January to October 2003. The measurement latitude coverage was 54–71°N and 64–88°S, which is similar to the coverage of ILAS (November 1996 to June 1997). One purpose of the ILAS-II measurements was to continue such high-latitude measurements of ozone and its related chemical species in order to help accurately determine their trends. The present paper assesses the quality of ozone data in the version 1.4 retrieval algorithm, through comparisons with results obtained from comprehensive ozonesonde measurements and four satellite-borne solar occultation sensors. In the Northern Hemisphere (NH), the ILAS-II ozone data agree with the other data within ±10% (in terms of the absolute difference divided by its mean value) at altitudes between 11 and 40 km, with the median coincident ILAS-II profiles being systematically up to 10% higher below 20 km and up to 10% lower between 21 and 40 km after screening possible suspicious retrievals. Above 41 km, the negative bias between the NH ILAS-II ozone data and the other data increases with increasing altitude and reaches 30% at 61–65 km. In the Southern Hemisphere, the ILAS-II ozone data agree with the other data within ±10% in the altitude range of 11–60 km, with the median coincident profiles being on average up to 10% higher below 20 km and up to 10% lower above 20 km.

[1]National Institute for Environmental Studies, Tsukuba, Japan.
[2]Graduate School of Environmental Studies, Nagoya University, Nagoya, Japan.
[3]Alfred Wegener Institute for Polar and Marine Research, Bremerhaven, Germany.
[4]Alfred Wegener Institute for Polar and Marine Research, Potsdam, Germany.
[5]National Institute of Polar Research, Tokyo, Japan.
[6]Central Aerological Observatory, Dolgoprudny, Russia.
[7]National Institute of Information and Communications Technology, Tokyo, Japan.
[8]Service d'Aéronomie, Centre National de la Recherche Scientifique, Paris, France.
[9]Service d'Aéronomie, Centre National de la Recherche Scientifique, Verrières-le-Buisson, France.
[10]British Antarctic Survey/Natural Environment Research Council, Cambridge, UK.
[11]Department of Atmospheric Science, University of Wyoming, Laramie, Wyoming, USA.
[12]Instituto Nacional de Técnica Aerospacial, Madrid, Spain.
[13]Finnish Meteorological Institute, Helsinki, Finland.
[14]Finnish Meteorological Institute, Sodankylä, Finland.

[15]NOAA Climate Monitoring and Diagnostics Laboratory, Boulder, Colorado, USA.
[16]Royal Netherlands Meteorological Institute, De Bilt, Netherlands.
[17]Institute of Meteorology and Water Management, Legionowo, Poland.
[18]Space and Atmospheric Sciences, Australian Antarctic Division, Kingston, Tasmania, Australia.
[19]Danish Meteorological Institute, Copenhagen, Denmark.
[20]Norwegian Institute for Air Research, Kjeller, Norway.
[21]Royal Meteorological Institute, Brussels, Belgium.
[22]Laboratory for Atmospheric and Space Physics, University of Colorado, Boulder, Colorado, USA.
[23]Remote Sensing Physics Branch, Naval Research Laboratory, Washington, D. C., USA.
[24]Science Systems and Applications, Inc., Lanham, Maryland, USA.
[25]NASA Langley Research Center, Hampton, Virginia, USA.
[26]Frontier Research Center for Global Change, Japan Agency for Marine-Earth Science and Technology, Yokohama, Japan.
[27]Now at Center for Atmospheric and Space Sciences, Utah State University, Logan, Utah, USA.
[28]Center for Climate System Research, University of Tokyo, Kashiwa, Japan.
[29]Division of Engineering and Applied Sciences, Harvard University, Cambridge, Massachusetts, USA.
[30]Central Research Institute of Electric Power Industry, Tokyo, Japan.

Considering the accuracy of the other data used for this comparative study, the version 1.4 ozone data are suitably used for quantitative analyses in the high-latitude stratosphere in both the Northern and Southern Hemisphere and in the lower mesosphere in the Southern Hemisphere.

1. Introduction

[2] The Improved Limb Atmospheric Spectrometer (ILAS)-II is a satellite-borne sensor that measures ozone and its related chemical species in the high-latitude stratosphere on the basis of the solar occultation technique [*Sasano et al.*, 2001; *Nakajima et al.*, 2006a]. ILAS-II is the successor to ILAS, which was continuously operated from November 1996 through June 1997 [*Sasano et al.*, 1995; *Sasano*, 2002, and references therein] and filled a gap between the Polar Ozone and Aerosol Measurement (POAM) II (October 1993 to November 1996) and POAM III (April 1998 to present) measurements. It is important to observe the vertical profile of ozone at high latitudes for several reasons: (1) to monitor ozone trends in the vertical distribution [e.g., *Randel and Wu*, 1999; *Staehelin et al.*, 2001]; (2) to evaluate the amount and/or rate of chemical ozone destruction in the polar vortex [e.g., *Bevilacqua et al.*, 1997; *Terao et al.*, 2002; *Hoppel et al.*, 2003; *Tilmes et al.*, 2003; *Singleton et al.*, 2005]; (3) to understand the impact of polar-processed air on midlatitude ozone [e.g., *Ajtić et al.*, 2004]; (4) to improve data assimilation of global three-dimensional ozone distribution [*Stajner and Wargan*, 2004]; (5) to improve the quality of ozone climatology data, hence, a priori information for data retrieval of nadir-viewing sensors [*Lamsal et al.*, 2004]; and (6) to predict the Arctic total ozone in the spring time using vertical profiles of ozone in the preceding Arctic fall [*Kawa et al.*, 2005].

[3] ILAS-II was launched onboard the Advanced Earth Observing Satellite (ADEOS)-II on 14 December 2002. It was preoperational between January and early April 2003, and then operational until the time ADEOS-II ceased operation on 24 October 2003 owing to a failure of the power supply of the satellite. During these periods, ILAS-II obtained 5890 observations, ranging in latitude from 54°N to 71°N and from 64°S to 88°S, depending on the season. There are approximately 14 measurements a day for each of the hemispheres, at sunrise seen from the satellite in the Northern Hemisphere (NH) and at sunset seen from the satellite in the Southern Hemisphere (SH). Local times at the Earth's surface are always p.m. in the NH, but in the SH they are a.m. between the end of March and the end of September, and p.m. at other times. Ranges of the measurement altitude (in the data files) of ozone are from 70 km to ~10 km. The lower limit varies from event to event, ranging down to 7 km, with a limiting factor of the sun tracking system (T. Tanaka et al., unpublished manuscript, 2006).

[4] In this paper, we focus on assessing the ILAS-II data quality of vertical profiles of ozone concentrations which were processed with the version 1.4 retrieval algorithm (the first public release). During the observation period, the four satellite solar occultation sensors, namely, the Stratospheric Aerosol and Gas Experiment (SAGE) II, SAGE III, the

Halogen Occultation Experiment (HALOE), and POAM III, were operational, so we used these data for comparisons. We used data from ozonesondes, which are valuable data for validation of ozone vertical profiles as an in situ measurement, although the comparisons are generally limited to the altitude range below 30–35 km. The ILAS-II comparison procedure is similar to that applied to ILAS, as described by *Sugita et al.* [2002].

2. ILAS-II: Instrumentation and Retrieval Algorithm

[5] ILAS-II mainly consists of the infrared channel (6.2–11.8 μm with 44 spectral elements) and the visible channel (753–784 nm with 1024 spectral elements), which were also used on ILAS. Two infrared channels (the midinfrared channel (3.0–5.7 μm with 22 spectral elements) and the other infrared channel (around 12.8 μm with 22 spectral elements)) are added in ILAS-II [*Nakajima et al.*, 2006a]. An improved version of the sun-edge sensor (SES) from that used in ILAS was also installed (T. Tanaka et al., unpublished manuscript, 2006). The υ_3 band centered near 9.6 μm in the infrared channel is used for detecting ozone. The data sampling rate of 10 Hz (i.e., data points with ancillary measurements every 0.1 s) is used for all channels and the SES. The instantaneous field of view at the tangent height (TH) has a 1 km height in the vertical direction and a 13 km width in the horizontal direction for the infrared channel. The partial slant path along the line of sight within a 1 km thick layer just above the TH of 20 km is less than 230 km. Applying a data smoothing digital filter for 21 consecutive data points, the vertical resolutions are estimated to be 1.3 km at a TH of 15 km and 2.9 km at a TH of 50 km, depending on atmospheric refraction (T. Yokota et al., unpublished manuscript, 2006).

[6] Vertical profiling of trace gases for ILAS-II adopts a method similar to that for ILAS as described by *Yokota et al.* [2002]. First, the retrieval algorithm is based on an "onion-peeling" method that uses a nonlinear least squares fitting for observed and theoretically calculated transmittance spectra (spectral fitting) from an altitude of 70 km to 10 km every 1 km downward to determine the volume mixing ratios (VMRs) of ten different trace gases (O_3, HNO_3, NO_2, N_2O, CH_4, H_2O, CFC-11, CFC-12, $ClONO_2$, and N_2O_5). The corresponding retrieval parameters are set to "unknown" parameters (target gases). The observed transmittance is derived from solar spectrum measurements (for 100% solar radiation calibration), deep space measurements (for 0% emission calibration), and each of the sampling data points through the atmosphere. The theoretically calculated transmittance is derived by determining a path length in the atmosphere for each of the data points

using a set of VMRs of target gases (as the initial guess, it is the same as the reference atmosphere model in section 3), absorption line parameters of these molecules, solar irradiance data, temperature and pressure profiles, and instrument functions of the infrared channel. In the version 1.4 retrieval algorithm, the High-resolution Transmission (HITRAN) 2000 edition including updates through 2001 [*Rothman et al.*, 2003] is used for the line parameters for gases. Pseudo line parameters provided by G. C. Toon (unpublished data, 1995, 2000) are used for $ClONO_2$, N_2O_5, CFC-11, and CFC-12. The CKD version 2.4 in the Line-By-Line Radiative Transfer Model (LBLRTM) [*Clough et al.*, 1989] is used for calculating the continuum absorption for H_2O. Temperature and pressure profiles required for the retrieval are taken from the United Kingdom Meteorological Office (Met Office, abbreviated here as MetO) stratospheric analyses data [*Swinbank and O'Neill*, 1994] implemented by the 3-D variational data assimilation scheme [*Lorenc et al.*, 2000] from 1000 hPa to 0.316 hPa and the COSPAR International Reference Atmosphere (CIRA) 1986 data [*Fleming et al.*, 1988] for the altitudes above the MetO data, and they are interpolated in time and space for each of the ILAS-II measurements for the retrieval. The version 1.4 algorithm is described in detail by T. Yokota et al. (unpublished manuscript, 2006).

3. ILAS-II: Error Analysis

[7] To evaluate the quality (in terms of precision) of the ILAS-II ozone retrieval itself is of importance, because if validation with other data shows a difference, we can judge whether the difference is really a bias or not. In the version 5.2 data of ILAS, two components of error are evaluated and then the total error is calculated by the root sum square (RSS) of each error [*Yokota et al.*, 2002]. One is an "internal error" which is determined by residuals in the spectral fitting procedure. The other is an "external error" which is determined by some sensitivity tests assuming uncertainties in data used for computing the calculated transmittance. It has been pointed out that the internal errors, which have been released as the ILAS data products, may involve systematic errors inherent in the calculated and/or observed spectra [*Yokota et al.*, 2002; *Toon et al.*, 2002], resulting in increased internal error values, particularly for minor gases: CFC-12 [*Khosrawi et al.*, 2004] and $ClONO_2$ [*Nakajima et al.*, 2006b]. Basically, internal errors are estimated on the basis of the assumption that spectral residuals are not systematic, and are due to random errors. Recently, however, an in-depth study on the spectral residuals has revealed that systematic spectral residuals of nonnegligible magnitude exist in the ILAS as well as in the ILAS-II measurement events in common (T. Yokota et al., unpublished manuscript, 2006). Therefore the internal error estimated for ILAS and ILAS-II data are overestimated as the random error, and should not be used for the index of random errors.

[8] Accordingly, instead of the conventional internal error calculations based on spectral residuals, "repeatability error" (see below) was employed as a measure of the random errors (or measurement precision) for processing the ILAS-II version 1.4 data products. Subsequently, external errors were calculated on the basis both of uncertainty in the
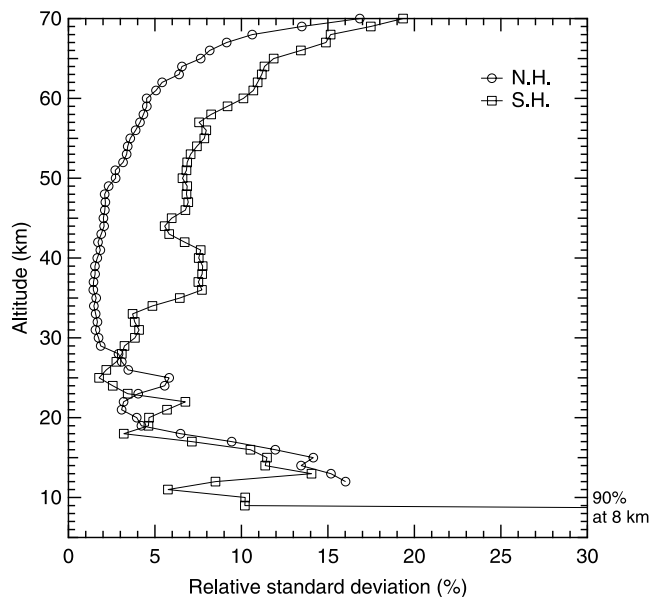

Figure 1. Profiles of the relative standard deviation for 100 consecutive occultation events in the most quiescent period during the ILAS-II measurements (see text, section 3).

assumed temperature, which had also been taken into consideration for the ILAS data retrievals, and uncertainty in the assumed climatological values of gas species, which is used for the nongaseous contribution correction method (see also below).

[9] A method for calculating the repeatability error, i.e., how to seek the "repeatability condition," is based on the minimum variability in VMRs found from the whole measurement period, instead of giving quiescent periods in advance as was done by *Yokota et al.* [2002] and *Khosrawi et al.* [2004]. In order to search for the most quiescent period, relative standard deviation (RSD) as one sigma standard deviation (around the mean) divided by the mean value was calculated for 100 consecutive occultation events (corresponding to about a 7.5 day period bin) at every 50 occultation events (corresponding to a time separation of about 3.5 days) repeatedly from April through October 2003 for both hemispheres. Profiles of the lowest RSDs in percent, which are considered to correspond to the most quiescent periods, are shown in Figure 1. Period bins that were selected at every altitude separately for both hemispheres are also shown in Table 1. Generally, the lowest RSD value is seen from the boreal summer and from the austral spring. This quantity represents an upper limit to the measurement precision, because it may also include real geophysical variability. In practice, the retrieval value (ppmv) multiplied by the fractional value of the lowest RSD is set to the repeatability error (ppmv) for all of the events separately for hemispheres in the ILAS-II version 1.4 data files. The derivation of the repeatability error is described in detail by T. Yokota et al. (unpublished manuscript, 2006). Finally, the total error was calculated from the RSS of the repeatability error and the external error, which was then incorporated in the ILAS-II version 1.4 data products. Note, however, that the total error

Table 1. Date of Selected Period Bins for Repeatability Calculations in 2003

Altitude, km	NH	SH	Altitude, km	NH	SH
8	. . .	19 Oct.			
9	. . .	5 Apr.			
10	. . .	8 Oct.			
11	. . .	1 Oct.	41	24 June	20 Sep.
12	9 Apr.	1 Oct.	42	24 June	16 Sep.
13	11 May	2 Sep.	43	12 July	16 Sep.
14	15 Sep.	2 Sep.	44	27 June	16 Sep.
15	8 July	5 Apr.	45	15 May	16 Sep.
16	24 Aug.	14 Aug.	46	13 June	16 Sep.
17	1 July	5 Apr.	47	15 May	5 Sep.
18	4 July	5 Apr.	48	15 May	5 Sep.
19	1 Sep.	15 May	49	15 May	5 Sep.
20	17 June	15 May	50	26 May	19 Oct.
21	8 May	15 May	51	26 May	19 Oct.
22	8 May	27 June	52	26 May	20 Sep.
23	11 May	1 Oct.	53	8 July	20 Sep.
24	11 May	16 Sep.	54	8 July	20 Sep.
25	8 July	16 Sep.	55	24 June	19 Oct.
26	29 July	13 Sep.	56	12 July	19 Oct.
27	29 July	2 Sep.	57	12 July	19 Oct.
28	27 June	22 Aug.	58	11 May	19 Oct.
29	27 June	27 June	59	17 June	19 Oct.
30	24 June	17 June	60	13 June	19 Oct.
31	24 June	17 June	61	10 Aug.	19 Oct.
32	24 June	17 June	62	22 May	19 Oct.
33	24 June	17 June	63	10 Aug.	19 Oct.
34	24 June	17 June	64	17 June	19 Oct.
35	27 June	17 June	65	12 July	19 Oct.
36	12 July	1 Oct.	66	24 June	19 Oct.
37	12 July	27 Sep.	67	8 July	19 Oct.
38	20 June	27 Sep.	68	17 June	19 Oct.
39	12 July	24 Sep.	69	17 June	19 Oct.
40	12 July	24 Sep.	70	27 June	19 Oct.

evaluated in this manner does not reflect the magnitude of spectral residuals in the spectral fitting.

[10] Two points should be noted in terms of uncertainties in the retrieved profiles, as discussed for the ILAS version 5.2 algorithm [*Yokota et al.*, 2002]. First, accuracy of the TH is crucial, because any TH ambiguity propagates directly to uncertainty in retrieved VMR profiles. For the ILAS-II version 1.4 algorithm, the TH was determined using the method discussed by T. Tanaka et al. (unpublished manuscript, 2006). The estimated accuracy in the determined TH is $180 \, m \pm 30 \, m$. Such an error will affect ozone VMRs by 2% at an altitude of 20 km and 5% at an altitude of 50 km (T. Tanaka et al., unpublished manuscript, 2006).

[11] The second point is the systematic errors associated with the nongaseous contribution correction by the simple linear interpolation between the window spectral elements

[*Yokota et al.*, 2002]. This method is still required in the ILAS-II version 1.4 algorithm in order to derive vertical profiles of the gaseous concentration in the altitude range where extinction due to aerosol particles (sulfate aerosols and/or polar stratospheric clouds, PSCs) cannot be neglected (T. Yokota et al., unpublished manuscript, 2006). To determine the nongaseous component in the theoretical calculation of the total (gaseous + nongaseous) transmittance, we calculate the nongaseous extinction coefficients at the four spectral elements where the absorption due to gaseous species is relatively small (so-called "window spectral element"). To do this, we used climatological values of gas VMR profiles (reference atmosphere model) as shown by T. Yokota et al. (unpublished manuscript, 2006) for calculating the gaseous contribution at the four spectral elements. The difference between the calculated (gaseous) and observed (gaseous + nongaseous) transmittances at the four spectral elements thus gives the nongaseous extinction coefficients by using the path length information. Finally, the nongaseous extinction coefficients at all the other 40 spectral elements can be derived by linear interpolation between these four window spectral elements, resulting in the nongaseous transmittance. Use of data from this reference atmosphere model would introduce some errors in the calculated transmittance at the four spectral elements; these are considered as the external error (as mentioned earlier). The interpolation would also produce systematic errors for the retrieved profiles of the gaseous concentration, but we do not include these in the external error. To evaluate them, we simulated transmittances for cases with several types of infrared absorption spectra for sulfate aerosols (50 and 75 wt% H_2SO_4/H_2O binary solutions) and PSCs (nitric acid trihydrate (NAT) particle, supercooled or liquid ternary solutions (STS or LTS) for four different compositions, and ice (ICE) particle) as nongaseous components and with the above mentioned reference profiles (a priori profiles) as gaseous components. Using these simulated transmittances, retrievals of the vertical profile of the gaseous concentration were made by applying the linear interpolation method for the nongaseous contribution in the version 1.4 retrieval algorithm discussed here. The difference between each set of the a priori and the retrieved gas profiles results in the systematic error. For convenience, the error is expressed in number density as a function of the aerosol extinction coefficient (AEC) at 780 nm data (which can be derived from the visible channel), and the result is shown by T. Yokota et al. (unpublished manuscript, 2006). Here, the systematic errors in terms of ozone VMR are listed in Table 2 for

Table 2. Summary of Possible Systematic Error in Ozone in ppmv Due to Aerosol/PSC Presence[a]

Altitude, km	AEC = 0.0005, km^{-1}		AEC = 0.001, km^{-1}					
	S(75)[b]	S(50)[b]	NAT	ICE	STS(5,37)[c]	STS(33,15)[c]	STS(47,3)[c]	STS(60,0.5)[c]
15	−0.01(−1)[d]	0.03(3)	0.04(4)	0.34(34)	<0.01(<1)	0.06(6)	0.07(7)	0.06(6)
20	−0.02(−1)[d]	0.06(2)	0.09(4)	0.74(30)	<0.01(<1)	0.14(6)	0.15(6)	0.13(5)
25	−0.03(−1)[d]	0.13(3)	0.20(5)	1.65(41)	<0.01(<1)	0.31(8)	0.33(8)	0.29(7)

[a]Systematic errors caused by the nongaseous component correction are listed for three selected altitudes. The error values at two selected aerosol extinction coefficients (AEC) at 780 nm are shown.

[b]S(75) and S(50) denote 75 and 50wt%-H_2SO_4/H_2O binary solutions, respectively.

[c]STS(5,37), STS(33,15), STS(47,3), and STS(60,0.5) denote 5, 33, 47, and 60wt%-H_2SO_4/37, 15, 3, and 0.5wt%-HNO_3/H_2O ternary solutions, respectively.

[d]Assuming ozone volume mixing ratios of 1.0, 2.5, and 4.0 ppmv at altitudes of 15, 20, and 25 km, respectively, percentage errors (%) are also shown in the parentheses.

Table 3. Summary of ECC Type Ozonesonde Measurements

Station	Latitude	Longitude	Number of Profiles	Principal Investigator
		ILAS-II Core Validation (ILAS-II CMDB)		
Kiruna[a]	67.9°N	21.1°E	7	H. Kanzawa
Syowa[b]	69.0°S	39.6°E	25	H. Kanzawa
		NICT Alaska Project (ILAS-II CMDB)		
Fairbanks	64.9°N	147.9°W	7	Y. Murayama
		QUOBI (Envisat Validation)		
De Bilt	52.1°N	5.2°E	5	M. Allaart
Legionowo	52.4°N	21.0°E	5	Z. Litynska
Ørland	63.4°N	9.2°E	3	G.O. Braathen
Salekhard[c]	66.7°N	66.7°E	4	V. Dorokhov/V.A. Yushkov
Scoresbysund	70.5°N	22.0°W	5	S.B. Andersen
Sodankylä	67.4°N	26.1°E	8	E. Kyrö
Uccle	50.8°N	4.4°E	3	H. De Backer
Yakutsk[c]	62.0°N	129.6°E	4	V. Dorokhov/V.A. Yushkov
Belgrano	77.9°S	34.6°W	11	M. Yela
Davis	68.6°S	78.0°E	5	A. Klekociuk
Dumont d'Urville	66.4°S	140.0°E	15	S. Godin-Beekmann, F. Goutail
Marambio	64.2°S	56.7°W	10	P. Taalas
McMurdo	77.9°S	166.7°E	12	T. Deshler
Neumayer[c]	70.4°S	8.2°W	15	G. Konig-Langlo/H. Gernandt
Rothera	67.6°S	68.1°W	13	H.K. Roscoe
South Pole	90.0°S	102.0°E	8	S.J. Oltmans, B.J. Johnson
Syowa[c]	69.0°S	39.6°E	11	K. Sato

[a]Data are also archived in the Envisat validation database.
[b]A RS II-KC-96 type sonde is used.
[c]Data are also archived in the ILAS-II CMDB.

the sulfate aerosols and the PSCs, assuming typical air number densities at altitudes of 15, 20 and 25 km.

4. Brief Description for Validation Data

4.1. SAGE II, SAGE III, HALOE, and POAM III

[12] In this analysis, we used ozone data from the SAGE II version 6.2 data, the SAGE III version 3 data, the HALOE version 19 data, and the POAM III version 4 data. All of the data are publicly available for scientific use through their World Wide Web servers (see Acknowledgments). The accuracy of the SAGE II version 6.2 ozone data is comparable to that of the version 6.1 ozone data where *Wang et al.* [2002] made comprehensive validation analyses. It reveals approximately 5% accuracy at altitudes between 15 and 45 km. *Taha et al.* [2004] confirmed that the SAGE III version 3 ozone data agree well with the SAGE II version 6.2 data within ±5% between 15 and 55 km. In this analysis, we used the RSS of this level of accuracy (5%) and random error values described in each SAGE II or III data file. For the HALOE version 19 ozone data, we used the RSS total error values that were estimated according to the procedure described by *Sugita et al.* [2002], on the basis of the HALOE error estimation from *Brühl et al.* [1996]. The POAM III version 3 ozone data reveals approximately 5% accuracy in altitudes between 13 and 60 km [*Randall et al.*, 2003]. For the POAM III version 4 ozone data, the difference from version 3 ozone data was evaluated to be less than 5% above 20 km in altitude. We used the RSS of this level of accuracy (5%) and random error values described in each POAM III data file.

4.2. Ozonesonde

[13] Table 3 shows a list of the number of ozonesonde profiles and the principal investigators (PI) for each of the

stations used here (see also section 5.1 for coincidence criteria). We used ozonesonde data from three nonpublic databases: one is the correlative measurement database (CMDB) of ILAS-II (http://www-ilas2.nies.go.jp/). The ILAS-II core validation was conducted at Kiruna, Sweden, and Syowa Station, Antarctica (PI: H. Kanzawa). The data from Fairbanks, Alaska (PI: Y. Murayama), have been taken as the Alaska Project led by the National Institute of Information and Communications Technology (NICT), Japan. The second is a database of the project Quantitative Understanding of Ozone losses by Bipolar Investigations (QUOBI) (http://www.nilu.no/quobi/). The third is the Envisat validation database (http://nadir.nilu.no/calval/). The Norwegian Institute for Air Research (NILU) maintains and manages the second and third databases. There are no differences in the ozone data between the QUOBI and Envisat databases for the same stations. Data from observations made at Neumayer (PI: G. König-Langlo/H. Gernandt) and Syowa Station (PI: K. Sato) in the Antarctic and Salekhard and Yakutsk in Russia (PI: V. Dorokhov/V. A. Yushkov) have been registered both in the QUOBI and CMDB databases. Data from observations made at Kiruna, Sweden, have been registered both in the CMDB and Envisat databases. The Electrochemical Concentration Cell (ECC) type ozonesondes [*Komhyr*, 1969] were used for all of the stations, except for Syowa Station (PI: H. Kanzawa) where observations were made using the RS II-KC-96 (KC) type sonde [*World Meteorological Organization (WMO)*, 1998, section 1.8] in addition to ECC type sondes (PI: K. Sato). The estimated precision and accuracy in the ECC ozonesonde measurements are ±3% and ±5%, respectively, in the stratosphere up to 10 hPa [*Komhyr et al.*, 1995]. According to *WMO* [1998, section 2.5], the systematic difference between different sonde

Table 4. Summary of Coincident Measurements of the Solar Occultation Sensors and Ozonesondes in 2003

					Occultation Mode[e]	
Period	Number[a]	Distance,[b] km	Time,[c] hours	Hemisphere[d]	ILAS-II	Others
ILAS-II-POAM III (Total Number = 1766, Criterion = 300 km/1 hour)						
Feb. to Oct.	632	168 (11)	0.2 (0.6, 0.0)	NH	SR	SR
Mar. to Oct.	1134	123 (13)	0.4 (1.0, 0.0)	SH	SS	SS
ILAS-II-SAGE III (Total Number = 213, Criterion = 300 km/1 hour)						
Apr., Aug., Sep.	213	204 (36)	0.2 (0.4, 0.0)	NH	SR	SS
ILAS-II-SAGE II (Total Number = 46, Criterion = 300 km/1 hours)						
Apr., July, Sep.	43	206 (29)	0.2 (0.4, 0.0)	NH	SR	SS, SS, SS
ILAS-II-HALOE (Total Number = 33, Criterion = 500 km/1 hour)						
May, Sep.	32	426 (279)	0.2 (0.7, 0.0)	NH	SR	SS, SS
Jan.	1	316	0.6	SH	SS	SS
ILAS-II-Ozonesondes (Total Number = 287, Criterion = 500 km/12 hours)						
Feb. to Oct.	51	326 (52)	4.5 (12, 0.0)	NH	SR	...
Feb., Apr. to Oct.	236	323 (63)	5.1 (12, 0.0)	SH	SS	...

[a]Numbers of coincident measurement pairs for each period (see also Figure 2).
[b]Average of individual distance between observed locations with respective separation criteria. Minimum distance is shown in parentheses.
[c]Average of individual absolute time difference between observation times with respective time criteria. Maximum and minimum time differences are shown in parentheses, respectively.
[d]SH and NH are for solar occultations occurring in the Southern Hemisphere and the Northern Hemisphere, respectively.
[e]SS and SR are for solar occultations occurring at sunset and sunrise as seen from the satellites, respectively.

types (including ECC and KC) is within ±5%, and the random variability is also smaller than 5%. In this analysis, we used an accuracy of 5% for altitudes below 30 km.

5. Comparative Conditions

5.1. Temporal and Spatial Criteria

[14] A conventional approach to making comparisons is used for this study, by seeking coincidence measurement pairs that fulfill certain criteria of temporal and spatial differences between the two. In order to compare ozone values in the upper stratosphere and lower mesosphere, a coincidence time criterion for satellite comparisons of 1 hour is used, since the diurnal variation of ozone in those altitude regions becomes significant above 50 km [e.g., *Brasseur and Solomon*, 1984]. We set the coincidence criteria basically to 300 km in distance. However, for comparisons with HALOE, 500 km is used for the distance criterion in order to increase the number of coincidence pairs. A list of the extracted pairs and the statistics is shown in Table 4. For comparisons with ozonesondes, we set the coincidence criteria to 500 km in distance and ±12 hours in time difference (same as *Sugita et al.* [2002]). A list of the stations and the number of profiles is already shown in Table 3, and the statistics is also shown in Table 4. In total, 176 ozonesonde profiles were extracted. As the representative location and time of the measurements, those at the measurement (or tangent) point of 20 km altitude were used. Movement of the balloon is considered for ozonesonde measurements using their wind data, if available, otherwise using the MetO wind data. Figures 2a and 2b show measurement latitudes at 20 km altitude of satellite sensors (order and color are corresponding to those for Figure 9) and ozonesondes used in this study, respectively.

5.2. Consistency of Altitude to Be Compared and Data Filtering

[15] In order to compare profiles between ILAS-II and validation data at every 1 km in geometric altitude, the vertical grids should be consistent with each other. Ozone data in a dimension of VMR or number density are provided in the vertical grid of 0.5 km for SAGE II and III, about 0.3 km for HALOE, 1 km for POAM III, and about 0.1 km for ozonesonde. The POAM III data are not necessary to be converted, but other data are converted into the 1 km grid by the method used by *Sugita et al.* [2002]. For the SAGE II and III data, ozone number densities were averaged at every 1 km using consecutive three data points centered at i km (i: integer), and then the VMR was calculated.

[16] To ensure consistency of the observed air masses, the data selection employed the method of *Sugita et al.* [2002] using the Ertel's potential vorticity (PV). PV values at every 1 km below 50 km in altitude were calculated by using the MetO data at each measurement location and time at 20 km altitude. We calculated relative differences in percent defined as:

$$100 \times 2 \times \{PV(ILAS\text{-}II) - PV(val)\}/\{PV(ILAS\text{-}II) + PV(val)\} \quad (1)$$

for each 1 km altitude grid point where PV(ILAS-II) and PV(val) denote PV values at the ILAS-II and validation measurement locations and times, respectively. The estimated uncertainty in the calculated PV values from the MetO data is roughly 3% on the basis of an examination of sensitivity. The PV difference by different vertical interpolations between linear and cubic-spline (cubic-spline is used here) in the potential temperature (PT) coordinate is about 2–3%. Differences of the PT at the same altitude are mostly less than 0.5%, correspond-
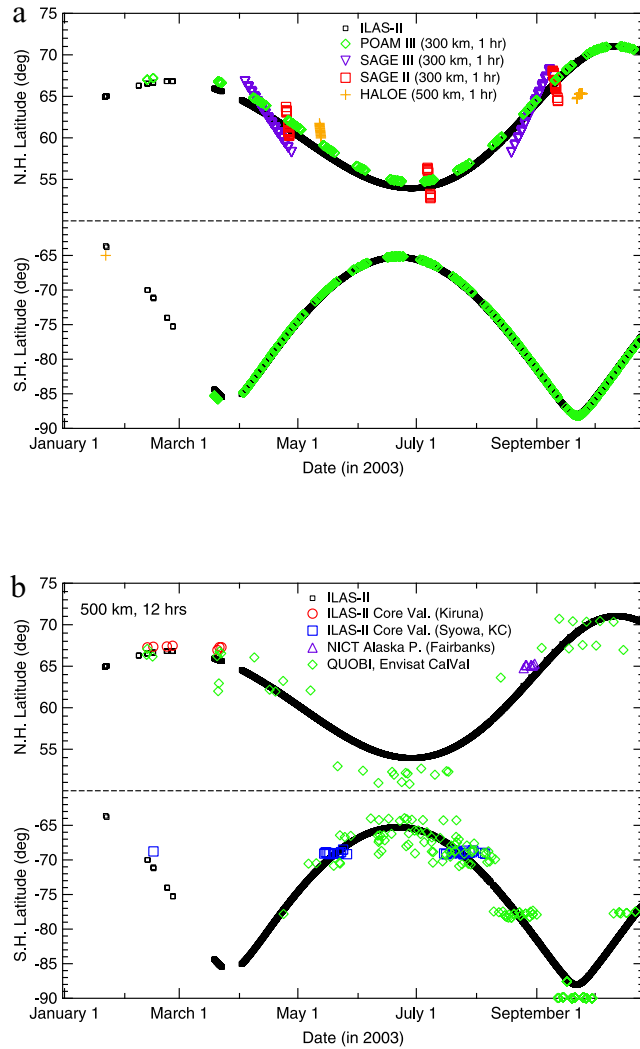
Figure 2. Latitudinal coverage of ILAS and locations (latitude) of the coincident measurements from (a) POAM III, SAGE III, HALOE, and SAGE II and (b) ozonesondes. See text (section 5.1) for coincidence criteria used in this study. Ozonesonde data were taken from the ILAS-II core validation experiment at Kiruna, Sweden, and at Syowa Station, Antarctica, and from the NICT Alaska project at Fairbanks, Alaska (see text, section 4.2). Two databases of QUOBI and Envisat validation were also used (see text, section 4.2).

ing to 2–3% differences of the PV values. If the difference exceeded ±15%, the data at these altitudes were discarded from this validation analysis. As a result, 318 (0.5% of the total number of altitudes below 50 km), 81 (1.0%), 113 (9.4%), and 230 (4.8%) number of altitudes are screened for comparisons with POAM III, SAGE III, HALOE, and ozonesondes, respectively, from this validation analysis.

[17] In this paper, we show the ILAS-II ozone data quality only using reliable retrievals, because we do not recommend data users to use possible suspicious data. We performed the data filtering as follows. If the ozone value

was less than the absolute value of its measurement uncertainty (as described in sections 3 and 4), the reliability of that ozone value was considered to be too low, and it was also filtered out. Moreover, as we discussed in section 3, the ILAS-II version 1.4 data might have been biased owing to the existence of aerosol/PSC. The possible biased ILAS-II ozone data were screened out as follows. As mentioned in section 3, the systematic error values can be estimated from the AEC at 780 nm data (T. Yokota et al., unpublished manuscript, 2006). The ILAS-II version 1.4 AEC at 780 nm data are validated elsewhere [*Saitoh et al.*, 2006]. The estimated systematic error for the ICE case, as an upper limit, at every altitude below 30 km is compared to the value equivalent to 15% of the retrieved value. If the former (systematic error) exceeded the latter, the data at these altitudes were discarded from this validation analysis. This is only effective for comparisons with POAM III and ozonesonde in the SH winter, since the AEC at 780 nm values are high owing to the presence of PSCs in those periods. Moreover, the lowermost stratospheric ozone data are also screened, yielding fewer coincidence pairs below 11 km especially in the NH. In addition, three profiles in the validation data (one from ozonesonde at South Pole Station, the others from HALOE and SAGE III) were discarded from this analysis, because they revealed apparently abnormal (or jagged) features.

6. Results and Discussion

6.1. Satellite Sensors

[18] In this subsection, we present the results of comparisons according to the number of correlative profiles, namely, POAM III, SAGE III, SAGE II, and then HALOE. Although the comparisons were made in both ozone number density and VMR, there is little difference in the results between the two approaches except for a comparison with HALOE shown in section 6.1.4. Therefore, to maintain consistency with *Sugita et al.* [2002] and the release format of the ILAS-II data (VMR), the comparison results are presented in VMR.

6.1.1. POAM III

[19] The left plots of Figures 3a and 3b illustrate average profiles of ozone measured by ILAS-II and POAM III for the measurement pairs listed in Table 4 in the NH and SH, respectively, together with several statistics relevant to the main results in the middle and right plots. In the right and middle plots, the median of individual absolute differences, AD, and relative differences, RD, between ILAS-II and POAM III are shown, respectively, together with several statistics. Here, AD and RD are defined as:

$$AD(ppmv) = O_3(ILAS\text{-}II) - O_3(val) \qquad (2)$$

$$RD(\%) = 100 \times 2 \times \{O_3(ILAS\text{-}II) - O_3(val)\}/\{O_3(ILAS\text{-}II) + O_3(val)\} \qquad (3)$$

where $O_3(ILAS\text{-}II)$ and $O_3(val)$ are ozone VMRs of ILAS-II and validation data (POAM III data in this case)
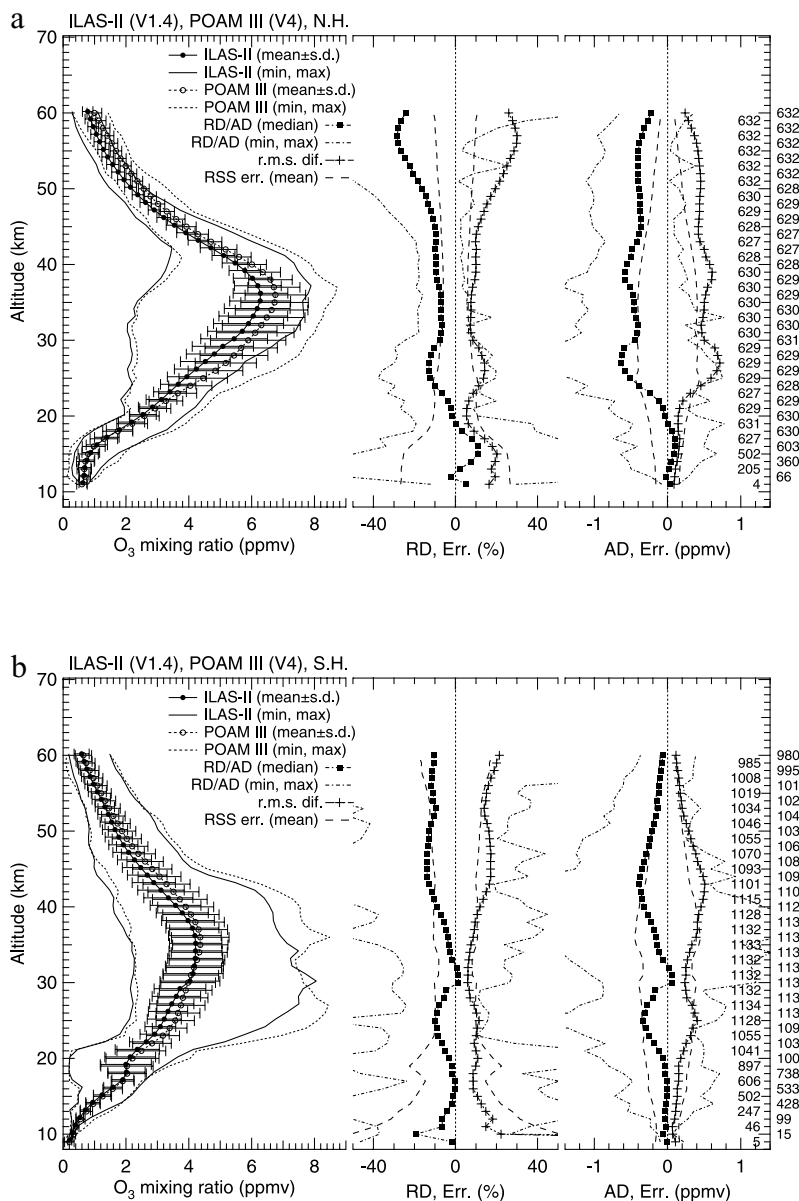
Figure 3. (a) Average profiles of ozone volume mixing ratios (VMRs) retrieved by ILAS-II and POAM III in the Northern Hemisphere (left plot) over the number of coincidence measurement pairs at each altitude. The ILAS data are plotted with 0.2 km shift for clarity. Error bars show one sigma standard deviation of the data at each altitude. Maximum and minimum values of the data are shown as a solid line (ILAS-II) and a dotted line (POAM III), respectively. Median profiles of individual percentage and absolute differences, labeled as RD and AD, respectively (see text for the definition), between ILAS-II and POAM III ozone VMRs are also shown (middle and right plots, respectively). Maximum and minimum values of the data are shown as dash-dotted lines. Root mean square (r.m.s.) difference of the data is also shown as a dash-dotted line with crosses. Dashed lines symmetrical with respect to the zero line show the average of individual root-sum-square total uncertainties, labeled as RSS err., in ILAS-II and POAM III measurements (see text). Numbers of coincidence measurement pairs at each altitude are shown on the right-hand side. (b) Same as Figure 3a but in the Southern Hemisphere.

at each geometric altitude grid point, respectively. Note that the above two equations (2) and (3) are also applied to any of the correlative data sources such as SAGE II, SAGE III, HALOE, or ozonesonde. The number, N, of coincidence measurement pairs at each altitude is shown on the right-hand side of Figure 3. Two dashed lines symmetrical with respect to the zero line show averages

of RSS of the errors in the ILAS-II and POAM III measurements at each altitude, defined as:

$$\text{Mean RSS error(\%)} = \sum_{i}^{N} \sqrt{\text{Err}_i(\text{ILAS-II})^2 + \text{Err}_i(\text{val})^2}/N$$

$$(i = 1 \text{ to } N) \qquad (4)$$
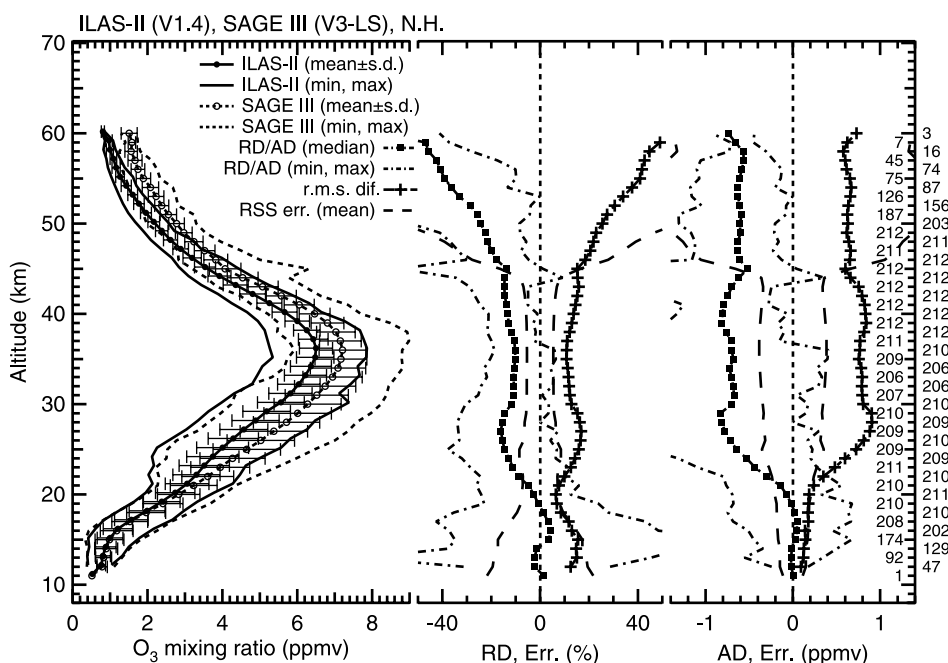
Figure 4. Same as Figure 3a but for ILAS-II and SAGE III (LS retrieval, "SAGE II like") in the Northern Hemisphere.

where Err(ILAS-II) and Err(val), respectively, show total measurement errors of ILAS-II and validation data, as described in sections 3 and 4, respectively. Note also that the above equation (4) is applied to any of the correlative data sources. The mean RSS error in the NH is within ±10% above 20 km in altitude, and increases to 30% below 20 km, whereas in the SH, the mean RSS error is several to 10% larger than that in the NH.

[20] In the NH comparison (Figure 3a), the median value of RD over N (middle plot) is within ±10% below 45 km, revealing a fairly good agreement, but decreases to near −30% with increasing altitudes above 45 km. The root mean square (r.m.s.) difference over N is roughly proportional to the absolute value of the median value, reaching 30% at the worst. Generally, the r.m.s. value is proportional to the absolute value of the median value for all of the comparisons in this paper as shown below. The median value of AD over N (right plot) is of the order of −0.4/−0.5 ppmv above 25 km. Below 25 km, the median value is near zero because of small retrieved values (left plot). In the SH comparison (Figure 3b), the median value of RD is roughly −10% for all altitudes. The median value of AD ranges from zero to −0.2 ppmv, reaching −0.4 ppmv at the worst (at 43 km).

[21] In comparisons with POAM III, we have a large number of pairs in each month in both of the hemispheres (see Figure 2a), and comparisons were made every month separately for the hemispheres. Although not shown in the figure, comparisons reveal that there is no significant seasonal dependence in the RD values for all altitude ranges.

6.1.2. SAGE III

[22] Figure 4 shows average profiles of ozone measured by ILAS-II and SAGE III in the NH. The SAGE III ozone values retrieved by the multiple linear regression (MLR) method and the least squares (LS) method (so-called "SAGE II like" retrieval) were compared with the ILAS-

II ozone values. Here, we used the LS retrieval for the SAGE III data, because the MLR ozone values are significantly higher than the LS ozone values up to 150% in the altitude range between 51 and 60 km. On the other hand, the MLR ozone values agree fairly well with the LS ozone values between 11 and 50 km (on average, the MLR ozone is 0.3% smaller than the LS ozone). The mean RSS error is within ±10% at altitudes between 20 and 40 km, but below and above the altitude range, it increases with increasing/decreasing altitude, reaching 20% at 11 km and 40% at 48 km. The median value of RD ranges from −10% to −20% between 23 and 47 km. Below 22 km, it ranges from −10% to +5%. The median value of AD ranges from −0.5 to −0.8 ppmv above 25 km, and it becomes near zero below 25 km. The RSS error increases significantly above 45 km, thus the significant negative deviations of the RD values up to −50% above 45 km are not conclusive.

[23] In Figure 5, retrievals from the mesospheric mode using the Hartley-Huggins band channel (284−296 nm) in the SAGE III data are compared to the ILAS-II data. In this comparison, information for the extracted measurement pairs differs somewhat from the comparison of the LS retrieval, since the representative location at an altitude of 50 km is used instead of that at 20 km (219 pairs in total were extracted). In Figure 5, we show the comparison above 50 km, below which the signal in the SAGE III Hartley-Huggins band channel is saturated. The median profile of RD reveals −30% above 55 km, exceeding the RSS error range of ±10−20%. The median profile of AD ranges from zero to −0.4 ppmv.

6.1.3. SAGE II

[24] Figure 6 shows average profiles of ozone measured by ILAS-II and SAGE II in the NH. The median profile of RD tends to decrease with increasing altitude, reaching −50% at altitudes above 65 km. The median value of AD
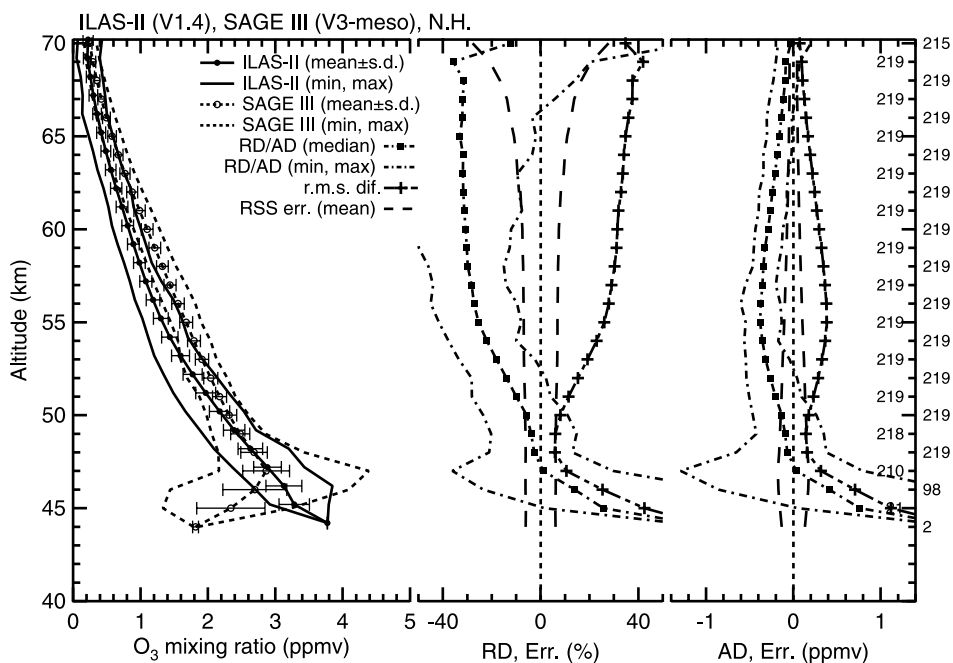
Figure 5. Same as Figure 3a but for ILAS-II and SAGE III (mesospheric mode) in the Northern Hemisphere. The altitude range is from 40 to 70 km.

is, on average, −0.4 to −0.5 ppmv above 25 km. It should be noted that the negative biases found above 50 km are roughly 10% larger than those found from other comparisons (ILAS-II and POAM III, SAGE III (mesospheric mode), or HALOE (see section 6.1.4)).

6.1.4. HALOE

[25] Figure 7a shows average profiles of ozone VMR measured by ILAS-II and HALOE in the NH. The median value of RD is within ±10% below 47 km, although it tends to decrease (the difference becomes large) with increasing

altitude. Such a tendency is remarkable above 48 km, reaching −40% at 68 km. The median value of AD is, on average, −0.6 ppmv at around 35–40 km, but it ranges from −0.4 to +0.1 ppmv for other altitudes. Figure 7b shows comparisons in ozone number density. It is interesting to note that the median value of RD in the number density comparison is from several to 10% (at maximum) lower than that in the VMR comparison above 30 km in altitude. This fact suggests that temperature and pressure data (and thus air number density) used for each of the
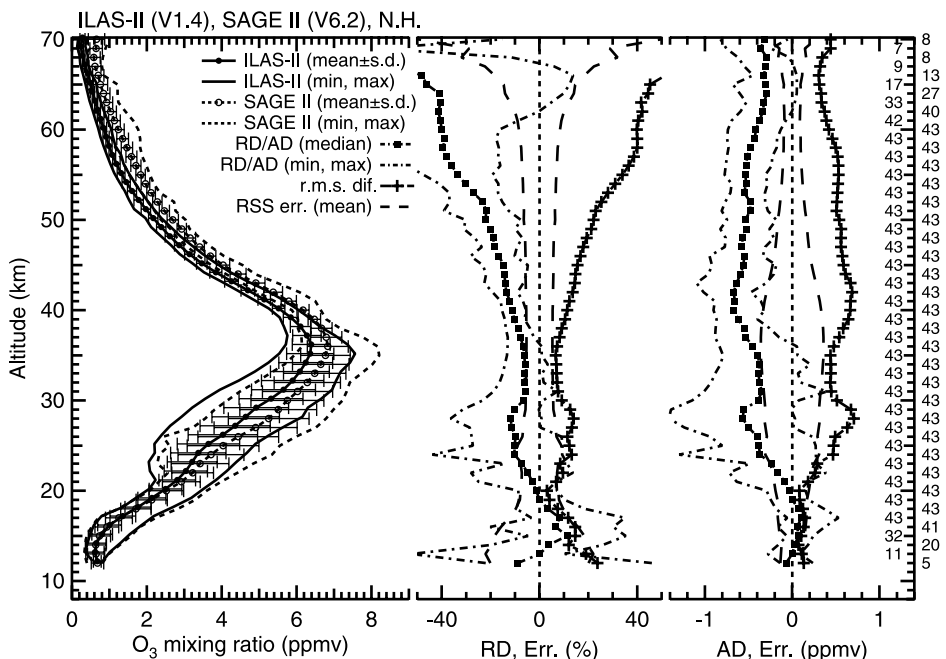
Figure 6. Same as Figure 3a but for ILAS-II and SAGE II in the Northern Hemisphere.
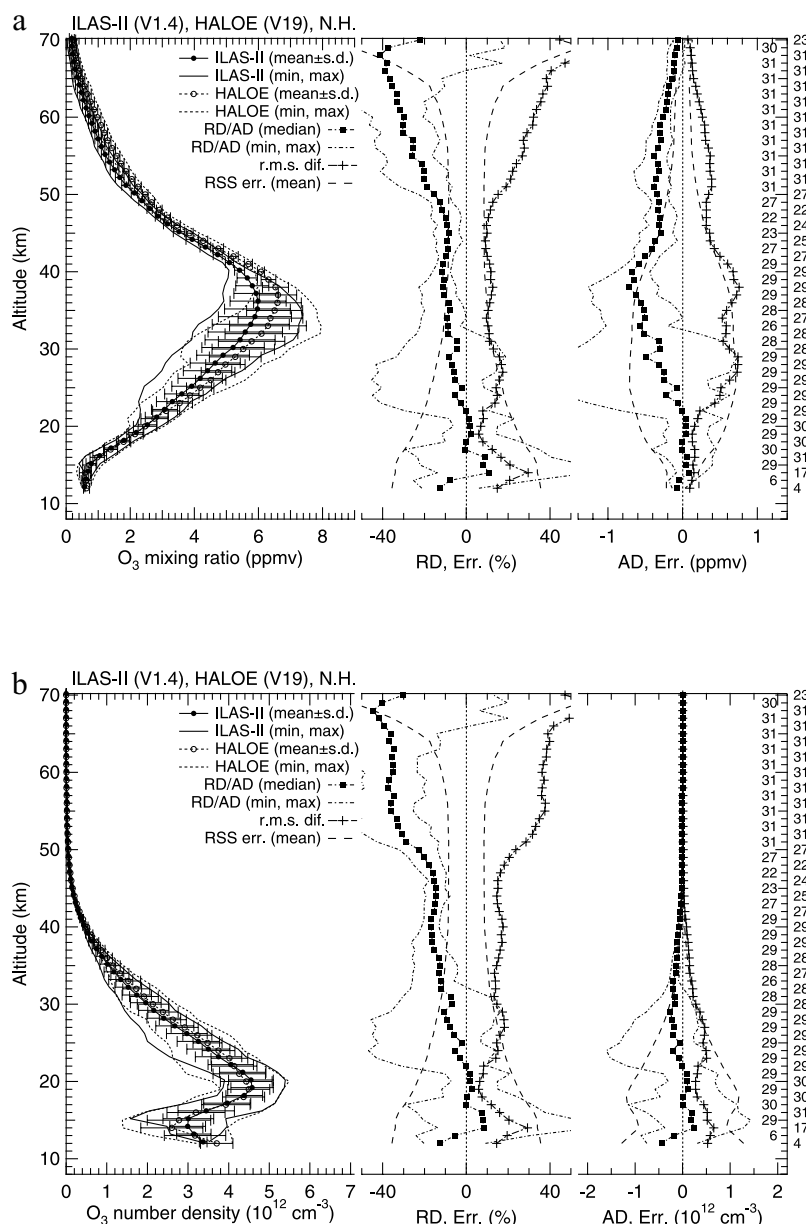
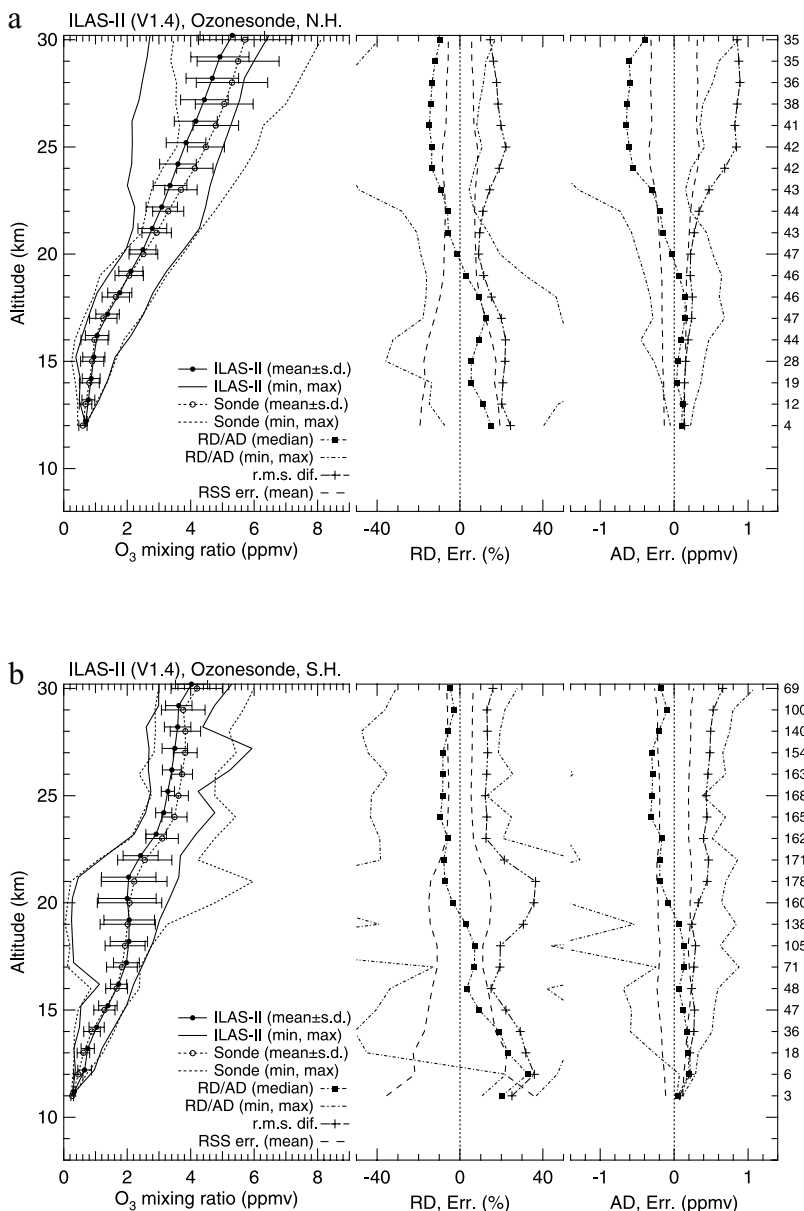**Figure 7.** (a) Same as Figure 3a but for ILAS-II and HALOE in the Northern Hemisphere. (b) Same as Figure 7a but in ozone number density.

retrieval algorithms are different at the same geometric altitude (ILAS-II uses the MetO and CIRA data, and HALOE uses its own retrievals). The differences in the temperature and pressure data may partly be due to the latitudinal difference of the measurements (see Figure 2a).

[26] Only one coincidence pair in the SH was found in January 2003 during the preoperational period of ILAS-II. Although not shown in figures such as Figure 7, there is no significant RD value of −30% at higher altitudes as was found in the NH comparisons. The result of the SH comparison will be illustrated in a summary figure (Figure 9) as a reference (see section 6.3).

6.2. Ozonesonde

[27] Similar to the satellite comparisons, comparisons with ozonesondes in VMR are described here. Note that

the difference between the comparison result in VMR and that in number density was at most a few percent. Average profiles of ozone measured by ILAS-II and ozonesondes in the NH below 30 km are shown in Figure 8a. Figure 8b shows average profiles of ozone measured by ILAS-II and ozonesondes in the SH. In total, 51 and 236 measurement pairs were used for the NH and SH comparisons from 51 and 124 vertical profiles of ozonesondes, respectively. Note that 93 coincidence pairs are used in this comparison from seven ozonesonde profiles at South Pole Station between 21 and 28 km (about 14 ILAS-II observations fulfill the coincidence criteria against only one ozonesonde observation). The inclusion of ozonesondes in the polar regions was particularly important, especially in the SH, because of the large chances of coincidence given by the ILAS-II orbit.

Figure 8. (a) Same as Figure 3a but for ILAS-II and ozonesondes in the Northern Hemisphere. (b) Same as Figure 3a but for ILAS-II and ozonesondes in the Southern Hemisphere.

[28] In the NH comparison, the median value of RD is within ±10%, but it can be seen that the RD values tend to be negative above and positive below a crossing point of 20 km altitude. The median value of AD is within ±0.2 ppmv below 20 km, but reaches −0.6 ppmv above 25 km. This is in accordance with results from the NH comparisons with both POAM III and SAGE II. Similar to the NH comparison, the median value of RD is negative (−5/−10%) above 20 km and positive (+30% at maximum) below 20 km in the SH comparison. However, the median value of AD shows much smaller deviation in the SH than in the NH, reaching −0.3 ppmv at most.

6.3. Summary for Each Data Source

[29] Using the results shown in sections 6.1 and 6.2, a statistical value, calculated by equation (5), is shown in

Figure 9. The median value of RD was averaged over each of the 5 km altitude bins, weighted by N at each altitude, for every validation source.

$$D(\text{weighted mean})(\%) = \Sigma(\text{RD}j \times \text{N}j)/\Sigma\text{N}j (j = 1 \text{ to } 5) \quad (5)$$

where j denotes each altitude within a 5 km altitude bin. For SAGE III, results from a comparison by the LS retrieval are shown below 60 km, and those by the mesospheric retrieval are shown above 51 km. For reference, ±10% guide lines are shown by dashed lines. In the NH comparisons (right plot), the D value is within +10% between 11 and 20 km, and within −10% between 21 and 40 km. We conclude that the sunrise mode ILAS-II data at 11−40 km have good accuracy, even though only five pairs were used at an altitude of 11 km. Above 41 km, the D value tends to
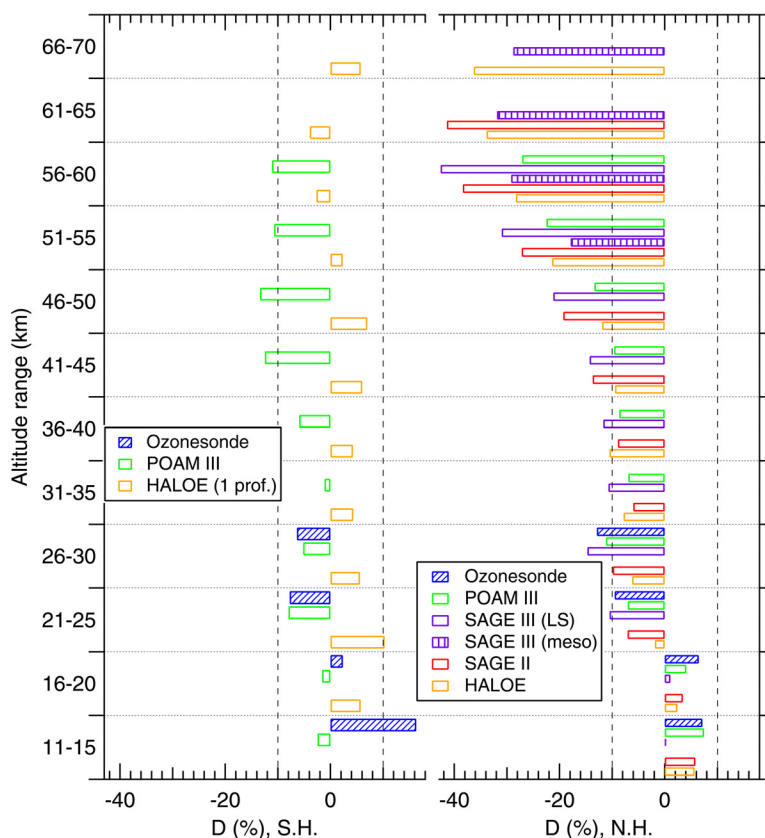
Figure 9. Average of the RD values for each 5 km altitude bin, weighted by the number of coincident pairs, from the results shown in Figures 3–8 (see text, section 6.3). Results for the Northern Hemisphere and the Southern Hemisphere (SH) are shown in the right and left plots, respectively. Note that only one coincidence measurement pair is used in the SH comparison for HALOE, which is shown as a reference.

decrease (smaller ILAS-II ozone values) with increasing altitude, although the magnitude of the D value is different according to the data sources. As discussed in section 6.1.2, the large negative deviations in the ILAS-II ozone data above 46 km found from comparison with SAGE III LS retrievals are not conclusive. Therefore we also conclude that the ILAS-II ozone data in the NH are 10–30% smaller (biased low) than others between 41 and 70 km, except for comparison with SAGE II from which the negative biases in the ILAS-II ozone data above 51 km are roughly 10% larger than those found from other comparisons.

[30] In the SH comparisons (left plot), it seems that there is no negative bias in the upper stratosphere/lower mesosphere as was found in the NH. Since only one profile was used for the SH comparison with HALOE, it is merely a reference for the SH statistical comparison. The result cannot be used to draw conclusions regarding the quality of ILAS-II ozone data. The D value is within ±10% for altitudes between 11 and 60 km, except for an 11–15 km bin (more than +10%), confirming a good accuracy of the sunset mode ILAS-II data.

[31] From the comparisons of ILAS-II ozone data with the other established data, the systematic negative bias found in the NH (sunrise mode) above 41 km suggests that there should be some unconsidered items in the current retrieval algorithm. The most possible item is an unresolved

problem in the measured signals due to a distortion in the entrance slit [*Nakajima et al.*, 2006a] which we did not expect before the launch. This feature is particularly evident above 40 km in the sunrise mode (owing probably to the difference in the measurement sequence of the sunrise mode compared to that of the sunset mode). Consequently, this affects retrieved vertical profiles of gas species to varying degrees, depending on gases and altitudes (or concentrations) (T. Yokota et al., unpublished manuscript, 2006). For instance, M. K. Ejiri et al. (Validation of Improved Limb Atmospheric Spectrometer (ILAS)-II version 1.4 nitrous oxide and methane profiles, submitted to *Journal of Geophysical Research*, 2005) reported a more negative bias even above 25 km in the CH_4 data than the ozone data in the NH. The retrieval algorithm of ILAS-II is still being updated, considering a correction method for the measured signals in the sunrise mode. After the update, a more accurate data set will be made public as was done in the ILAS version 5.2 data set [*Sasano*, 2002, and references therein] from the ILAS version 3.1 data set [*Sasano et al.*, 1999, and references therein].

7. Concluding Remarks

[32] As the successor to ILAS for high-latitude stratospheric observation (from October 1996 to June 1997), a

solar occultation sensor, ILAS-II, was launched on board ADEOS-II in December 2002. Unfortunately, like ILAS, ILAS-II ceased operation within the year after launch in October 2003 because of a failure in the power supply of the satellite. From January to October 2003, ILAS-II measured 5890 vertical profiles of ozone concentrations between 7 and 70 km. Assessment of ILAS-II ozone data quality in the version 1.4 retrieval algorithm was made through comparisons with coincident measurements of ozonesonde and four satellite-borne solar occultation sensors.

[33] The ILAS-II ozone data in the NH between 11 and 40 km agree with the other data within ±10% (in terms of the absolute difference divided by its mean value) for most cases, with the median coincident ILAS-II profiles being systematically up to 10% higher below 20 km and up to 10% lower between 21 and 40 km after screening possible suspicious retrievals. Above 41 km, the negative bias between the NH ILAS-II ozone data and the other data increases with increasing altitude and reaches 30% at 61–65 km. In the SH, the ILAS-II ozone data agree with the other data within ±10% in the altitude range of 11–60 km, with the median coincident profiles being on average up to 10% higher below 20 km and up to 10% lower above 20 km. Considering the accuracy of the other data used for this comparative study, the version 1.4 ozone data are suitable for quantitative analyses in the NH between 11 and 40 km and in the SH between 11 and 70 km.

References

Ajtić, J., B. J. Connor, B. N. Lawrence, G. E. Bodeker, K. W. Hoppel, J. E. Rosenfield, and D. N. Heuff (2004), Dilution of the Antarctic ozone hole into southern midlatitudes, 1998–2000, *J. Geophys. Res.*, *109*, D17107, doi:10.1029/2003JD004500.

Bevilacqua, R. M., et al. (1997), POAM II ozone observations in the Antarctic ozone hole in 1994, 1995 and 1996, *J. Geophys. Res.*, *102*(D19), 23,643–23,658.

Brasseur, G., and S. Solomon (1984), *Aeronomy of the Middle Atmosphere*, 441 pp., Springer, New York.

Brühl, C., et al. (1996), Halogen Occultation Experiment ozone channel validation, *J. Geophys. Res.*, *101*(D6), 10,217–10,240.

Clough, S. A., F. X. Kneizys, and R. W. Davis (1989), Line shape and the water vapor continuum, *Atmos. Res.*, *23*, 229–241.

Fleming, E. L., S. Chandra, M. R. Shoeberl, and J. J. Barnett (1988), Monthly mean global climatology of temperature, wind, geopotential height and pressure for 0–120 km, *NASA Tech. Memo. 100697*.

Hoppel, K., R. Bevilacqua, D. Allen, G. Nedoluha, and C. Randall (2003), POAM III observations of the anomalous 2002 Antarctic ozone hole, *Geophys. Res. Lett.*, *30*(7), 1394, doi:10.1029/2003GL016899.

Kawa, S. R., P. A. Newman, R. S. Stolarski, and R. M. Bevilacqua (2005), Fall vortex ozone as a predictor of springtime total ozone at high northern latitudes, *Atmos. Chem. Phys.*, *5*, 1655–1663.

Khosrawi, F., et al. (2004), Validation of CFC-12 measurements from the Improved Limb Atmospheric Spectrometer (ILAS) with the version 6.0 retrieval algorithm, *J. Geophys. Res.*, *109*, D06311, doi:10.1029/2003JD004325.

Komhyr, W. D. (1969), Electrochemical concentration cells for gas analysis, *Ann. Geophys.*, *25*, 203–210.

Komhyr, W. D., R. A. Barnes, G. B. Brothers, J. A. Lathrop, and D. P. Opperman (1995), Electrochemical concentration cell ozonesonde performance evaluation during STOIC 1989, *J. Geophys. Res.*, *100*(D5), 9231–9244.

Lamsal, L. N., M. Weber, S. Tellmann, and J. P. Burrows (2004), Ozone column classified climatology of ozone and temperature profiles based on ozonesonde and satellite data, *J. Geophys. Res.*, *109*, D20304, doi:10.1029/2004JD004680.

Lorenc, A. C., et al. (2000), The Met Office global three-dimensional variational data assimilation scheme, *Q. J. R. Meteorol. Soc.*, *126*(570), 2991–3012.

Nakajima, H., et al. (2006a), Characteristics and performance of the Improved Limb Atmospheric Spectrometer-II (ILAS-II) onboard the ADEOS-II satellite, *J. Geophys. Res.*, doi:10.1029/2005JD006334, in press.

Nakajima, H., et al. (2006b), Measurements of ClONO$_2$ by the Improved Limb Atmospheric Spectrometer (ILAS) in high-latitude stratosphere: New products using version 6.1 data processing algorithm, *J. Geophys. Res.*, doi:10.1029/2005JD006441, in press.

Randall, C. E., et al. (2003), Validation of POAM III ozone: Comparisons with ozonesonde and satellite data, *J. Geophys. Res.*, *108*(D12), 4367, doi:10.1029/2002JD002944.

Randel, W. J., and F. Wu (1999), A stratospheric ozone trends data set for global modeling studies, *Geophys. Res. Lett.*, *26*(20), 3089–3092.

Rothman, L. S., et al. (2003), The HITRAN molecular spectroscopic database: Edition of 2000 including updates through 2001, *J. Quant. Spectrosc. Radiat. Transfer*, *82*(1–4), 5–44.

Saitoh, N., et al. (2006), Intercomparison of ILAS-II version 1.4 aerosol extinction coefficients at 780 nm with those from SAGE II, SAGE III, and POAM III, *J. Geophys. Res.*, doi:10.1029/2005JD006315, in press.

Sasano, Y. (2002), Preface, *J. Geophys. Res.*, *107*(D24), 8204, doi:10.1029/2002JD002155.

Sasano, Y., M. Suzuki, T. Yokota, and H. Kanzawa (1995), Improved Limb Atmospheric Spectrometer (ILAS) project: ILAS instrument, performance and validation plan, *Proc. SPIE*, *2583*, 193–204.

Sasano, Y., et al. (1999), Validation of ILAS version 3.10 ozone with ozonesonde measurements, *Geophys. Res. Lett.*, *26*(7), 831–834.

Sasano, Y., T. Yokota, H. Nakajima, T. Sugita, and H. Kanzawa (2001), ILAS-II instrument and data processing system for stratospheric ozone layer monitoring, 9–12 October 2000, Sendai, Japan, *Proc. SPIE*, *4150*, 106–114.

Singleton, C. S., C. E. Randall, M. P. Chipperfield, S. Davies, W. Feng, R. M. Bevilacqua, K. W. Hoppel, M. D. Fromm, G. L. Manney, and V. L. Harvey (2005), 2002–2003 Arctic ozone loss deduced from POAM III satellite observations and the SLIMCAT chemical transport model, *Atmos. Chem. Phys.*, *5*, 597–609.

Staehelin, J., N. R. P. Harris, C. Appenzeller, and J. Eberhard (2001), Ozone trends: A review, *Rev. Geophys.*, *39*(2), 231–290.

Stajner, I., and K. Wargan (2004), Antarctic stratospheric ozone from the assimilation of occultation data, *Geophys. Res. Lett.*, *31*, L18108, doi:10.1029/2004GL020846.

Sugita, T., et al. (2002), Validation of ozone measurements from the Improved Limb Atmospheric Spectrometer, *J. Geophys. Res.*, *107*(D24), 8212, doi:10.1029/2001JD000602.

Swinbank, R., and A. O'Neill (1994), A stratosphere-troposphere data assimilation system, *Mon. Weather Rev.*, *122*, 686–702.

Taha, G., L. W. Thomason, C. Trepte, and W. P. Chu (2004), Validation of SAGE III data products version 3.0, paper presented at Quadrennial

Ozone Symposium, Int. Ozone. Comm., Int. Assoc. for Meteorol. and Atmos. Sci., Kos, Greece, 1–8 Sept.

Terao, Y., Y. Sasano, H. Nakajima, H. L. Tanaka, and T. Yasunari (2002), Stratospheric ozone loss in the 1996/1997 Arctic winter: Evaluation based on multiple trajectory analysis for double-sounded air parcels by ILAS, *J. Geophys. Res.*, *107*(D24), 8210, doi:10.1029/2001JD000615.

Tilmes, S., R. Müller, J.-U. Grooss, D. S. McKenna, J. M. Russell III, and Y. Sasano (2003), Calculation of chemical ozone loss in the Arctic winter 1996–1997 using ozone-tracer correlations: Comparison of Improved Limb Atmospheric Spectrometer (ILAS) and Halogen Occultation Experiment (HALOE) results, *J. Geophys. Res.*, *108*(D2), 4045, doi:10.1029/2002JD002213.

Toon, G., B. Sen, J.-F. Blavier, Y. Sasano, T. Yokota, H. Kanzawa, T. Ogawa, M. Suzuki, and K. Shibasaki (2002), Comparison of ILAS and MkIV profiles of atmospheric trace gases measured above Alaska in May 1997, *J. Geophys. Res.*, *107*(D24), 8211, doi:10.1029/2001JD000640.

Wang, H. J., D. M. Cunnold, L. W. Thomason, J. M. Zawodny, and G. E. Bodeker (2002), Assessment of SAGE version 6.1 ozone data quality, *J. Geophys. Res.*, *107*(D23), 4691, doi:10.1029/2002JD002418.

World Meteorological Organization (1998), Assessment of trends in the vertical distribution of ozone, *SPARC Rep. 1*, Global Ozone Res. and Monit. Proj., Geneva, Switzerland.

Yokota, T., H. Nakajima, T. Sugita, H. Tsubaki, Y. Itou, M. Kaji, M. Suzuki, H. Kanzawa, J. H. Park, and Y. Sasano (2002), Improved Limb Atmospheric Spectrometer (ILAS) data retrieval algorithm for version 5.20 gas profile products, *J. Geophys. Res.*, *107*(D24), 8216, doi:10.1029/2001JD000628.

————————————

M. Allaart, Royal Netherlands Meteorological Institute, DK-3730 AE De Bilt, Netherlands.

S. B. Andersen, Danish Meteorological Institute, DK-2100 Copenhagen, Denmark.

R. M. Bevilacqua, Remote Sensing Physics Branch, Naval Research Laboratory, Washington, DC 20375, USA.

G. O. Braathen, Norwegian Institute for Air Research, N-2027 Kjeller, Norway.

H. De Backer, Royal Meteorological Institute, B-1000 Brussels, Belgium.

T. Deshler, Department of Atmospheric Science, University of Wyoming, Laramie, WY 82071, USA.

V. Dorokhov and V. A. Yushkov, Central Aerological Observatory, 3, Pervomayskaya str., Dolgoprudny, Moscow Region 141700, Russia.

M. K. Ejiri, Center for Atmospheric and Space Sciences, Utah State University, Logan, UT 84322, USA.

H. Gernandt, A. Herber, and G. König-Langlo, Alfred Wegener Institute for Polar and Marine Research, D-27515 Bremerhaven, Germany.

S. Godin-Beekmann, Service d'Aéronomie, Centre National de la Recherche Scientifique, F-75252 Paris, France.

F. Goutail, Service d'Aéronomie, Centre National de la Recherche Scientifique, BP 3, Route des Gatines, F-91370 Verrières-le-Buisson, France.

H. Irie, Frontier Research Center for Global Change, Japan Agency for Marine-Earth Science and Technology, Yokohama 236-0001, Japan.

B. J. Johnson and S. J. Oltmans, NOAA Climate Monitoring and Diagnostics Laboratory, Boulder, CO 80305, USA.

H. Kanzawa, Graduate School of Environmental Studies, Nagoya University, Nagoya 464-8601, Japan.

A. Klekociuk, Space and Atmospheric Sciences, Australian Antarctic Division, Kingston, Tas 7050, Australia.

H. Kobayashi, Central Research Institute of Electric Power Industry, Otemachi, Chiyoda-ku, Tokyo 100-8126, Japan.

E. Kyrö, Finnish Meteorological Institute, FI-99600 Sodankylä, Finland.

Z. Litynska, Institute of Meteorology and Water Management, PL-05119 Legionowo, Poland.

Y. Murayama and M. Yamamori, National Institute of Information and Communications Technology, Koganei, Tokyo 184-8795, Japan.

H. Nakajima, Y. Sasano, T. Sugita, T. Tanaka, and T. Yokota, National Institute for Environmental Studies, Tsukuba 305-0053, Japan. (tsugita@nies.go.jp)

C. E. Randall, Laboratory for Atmospheric and Space Physics, University of Colorado, Boulder, CO 80303, USA.

H. K. Roscoe, British Antarctic Survey/Natural Environment Research Council, Cambridge CB3 0ET, UK.

N. Saitoh, Center for Climate System Research, University of Tokyo, Kashiwa 277-8568, Japan.

K. Sato, National Institute of Polar Research, Tokyo 173-8515, Japan.

P. Taalas, Finnish Meteorological Institute, FI-00101 Helsinki, Finland.

G. Taha, Science Systems and Applications, Inc., Lanham, MD 20706, USA.

Y. Terao, Division of Engineering and Applied Sciences, Harvard University, Cambridge, MA 02138, USA.

L. W. Thomason, NASA Langley Research Center, Hampton, VA 23681, USA.

P. von der Gathen, Alfred Wegener Institute for Polar and Marine Research, Telegrafenberg A43, D-14473 Potsdam, Germany.

M. Yela, Instituto Nacional de Técnica Aeroespacial, Ctra. De Ajalvir km 4, E-28850 Madrid, Spain.